

## Dynamical structure factor of the $J_1$ - $J_2$ Heisenberg model in one dimension: The variational Monte Carlo approach

Francesco Ferrari,<sup>1,\*</sup> Alberto Parola,<sup>2</sup> Sandro Sorella,<sup>1</sup> and Federico Becca<sup>3</sup>

<sup>1</sup>*International School for Advanced Studies (SISSA), Via Bonomea 265, I-34136 Trieste, Italy*

<sup>2</sup>*Dipartimento di Scienza e Alta Tecnologia, Università dell'Insubria, Via Valleggio 11, I-22100 Como, Italy*

<sup>3</sup>*Democritos National Simulation Center, Istituto Officina dei Materiali del CNR and International School for Advanced Studies (SISSA), Via Bonomea 265, I-34136 Trieste, Italy*



(Received 14 March 2018; revised manuscript received 18 May 2018; published 5 June 2018)

The dynamical spin structure factor is computed within a variational framework to study the one-dimensional  $J_1$ - $J_2$  Heisenberg model. Starting from Gutzwiller-projected fermionic wave functions, the low-energy spectrum is constructed from two-spinon excitations. The direct comparison with Lanczos calculations on small clusters demonstrates the excellent description of both gapless and gapped (dimerized) phases, including incommensurate structures for  $J_2/J_1 > 0.5$ . Calculations on large clusters show how the intensity evolves when increasing the frustrating ratio and give an unprecedented accurate characterization of the dynamical properties of (nonintegrable) frustrated spin models.

DOI: [10.1103/PhysRevB.97.235103](https://doi.org/10.1103/PhysRevB.97.235103)

### I. INTRODUCTION

Quantum spin liquids are unconventional phases of matter in which quantum fluctuations endure any tendency to develop local (e.g., magnetic) order, down to zero temperature. Most importantly, the lack of any symmetry-breaking mechanism is accompanied by topological order and the presence of excitations with fractional quantum numbers [1]. For concreteness, let us consider the spin-1/2 Heisenberg model on a given two-dimensional lattice. Whenever magnetic order sets in (e.g., on the square lattice with nearest-neighbor antiferromagnetic interactions), the elementary excitations are  $S = 1$  magnons or spin waves, which can be pictured as coherent Bloch waves made from localized spin-flip excitations. Instead, in spin liquids, the elementary objects are  $S = 1/2$  spinons, while  $S = 1$  excitations decay in two spinons that are asymptotically free at long distances [1]. Since, for any lattice with a fixed number of sites, the minimal change in the total spin is  $\Delta S = \pm 1$ , the existence of objects with  $S = 1/2$  implies a fractionalization of the spin quantum number. Spinons do exist in the one-dimensional Heisenberg model [2], where the magnetic long-range order is hampered, in agreement with the generalized Mermin-Wagner theorem [3]. In this case, the spectrum is gapless and characterized by the presence of a broad continuum of excitations. A similar feature is present in the one-dimensional Heisenberg model with inverse-square superexchange [4]; in this case, spinons are noninteracting, and the whole excitation spectrum can be found explicitly in a closed form [5]. Moreover,  $S = 1/2$  objects are elementary excitations also in gapped systems, as in the case of the Majumdar-Ghosh point of the frustrated  $J_1$ - $J_2$  Heisenberg model (where the ratio between the first-neighbor coupling  $J_1$  and the second-neighbor one  $J_2$  is equal to 2). Here, the ground

state is doubly degenerate (with long-range dimer order) [6], and elementary excitations can be seen as propagating defect boundaries between the two ground states (they are analogous to solitons) [7]. Anyhow, in one-dimensional systems, fractional excitations are ubiquitous and represent the general feature of spin models. By contrast, in two spatial dimensions, neat examples of spin liquids are rarer, and the possibility to have free (i.e., deconfined) spinons when magnetic order is destroyed is not taken for granted. A beautiful example in which fractional excitations are present is given by the Kitaev (compass) model on the honeycomb lattice [8], where elementary excitations are Majorana fermions and  $Z_2$  gauge fluxes.

In the last 20 years, a huge effort has been devoted to assessing the low-energy behavior of various frustrated spin models in order to unveil possible spin-liquid ground states. Many different lattice structures and various kinds of interactions, including long-range superexchange and ring-exchange terms, have been considered by employing a large variety of analytical and numerical techniques [9]. Nevertheless, most of these studies focused on the ground-state properties by computing correlation functions or different quantities that may give information about the presence or absence of a spin gap. The direct computation of the spin gap has been performed in a few cases, notably for the Heisenberg model on the kagome lattice, where this issue has been addressed using the density-matrix renormalization group [10,11], variational Monte Carlo [12], and Lanczos [13] approaches. By contrast, only a few works, mainly based upon analytical or semianalytical approaches, have focused on all the dynamical properties of frustrated spin models [14–17]. In this respect, an important quantity that gives direct access to the nature of the excitation spectrum is the dynamical structure factor:

$$S^a(q, \omega) = \sum_{\alpha} |\langle \Upsilon_{\alpha}^q | S_q^a | \Upsilon_0 \rangle|^2 \delta(\omega - E_{\alpha}^q + E_0), \quad (1)$$

\*frferra@sisssa.it

where  $|\Upsilon_0\rangle$  is the ground state of the system with energy  $E_0$ ,  $\{|\Upsilon_\alpha^q\rangle\}$  are the excited states with momentum  $q$  (relative to the ground state) and energy  $E_\alpha^q$ , and

$$S_q^a = \frac{1}{\sqrt{L}} \sum_R e^{iqR} S_R^a \quad (2)$$

is the Fourier-transformed spin operator for the components  $a = (x, y, z)$ , with  $L$  being the number of sites of the cluster. In this regard, inelastic neutron scattering provides a direct measurement of the dynamical structure factor as a function of momentum  $q$  and energy  $\omega$ . Therefore, the theoretical computation of  $S^a(q, \omega)$  has an immediate connection to experiments, thus validating or disproving the modelization of a given real material [18–20].

Unfortunately, the theoretical evaluation of the dynamical structure factor is possible only for very limited cases. In one dimension, an exact calculation is possible for the Heisenberg model with inverse-square superexchange [21], while very accurate approximations are now available for the simple Heisenberg model with nearest-neighbor interaction [22–24]. In two spatial dimensions, an exact computation of the dynamical structure factor is possible for the Kitaev model in both the gapless and gapped regimes [25]. Besides these fortunate cases in which the model is integrable, numerical techniques have been employed to study generic models, especially in one dimension. Here, exact diagonalizations can be performed on relatively small clusters [26], and their results can be compared with semianalytical calculations [27]. Moreover, the density-matrix renormalization group [28] or matrix-product states [29,30] can be used. Alternatively, a variational technique, implemented within a quantum Monte Carlo method, has been suggested to approximate the exact spectrum with  $L$  states for each momentum  $q$  [31]. The important advantage of this approach is that the dynamical structure factor  $S(q, \omega)$  is directly accessible, without any computation requiring (unstable) transformations from real or imaginary times to frequencies [32]. Curiously, this approach has been applied in very few cases [33,34], without systematic benchmarks and comparisons with other methods.

In this paper, we employ the variational approach that was introduced in Ref. [31] to compute the dynamical structure factor of Eq. (1) for momentum  $q$  and energy  $\omega$  in the spin-1/2  $J_1$ - $J_2$  Heisenberg model in one dimension:

$$\mathcal{H} = J_1 \sum_R \mathbf{S}_R \cdot \mathbf{S}_{R+1} + J_2 \sum_R \mathbf{S}_R \cdot \mathbf{S}_{R+2}, \quad (3)$$

where  $R = 1, 2, \dots, L$  are the (integer) coordinates of the  $L$  sites and  $\mathbf{S}_R = (S_R^x, S_R^y, S_R^z)$  is the  $S = 1/2$  spin operator on site  $R$ . Periodic boundary conditions are considered in the spin Hamiltonian. In the following, we will consider the case with  $a \equiv z$  in Eq. (1) since, given the  $SU(2)$  symmetry of the Heisenberg model, any component of the structure factor gives the same result. The variational Monte Carlo results are compared with Lanczos diagonalizations on a small  $L = 30$  cluster in order to show the accuracy of the method for different values of the frustrating ratio  $J_2/J_1$ . Then, calculations are reported for large systems, illustrating how the various features of the dynamical structure factor evolve from the gapless to the

gapped phase, also entering in the incommensurate region with  $J_2/J_1 > 0.5$ .

The rest of the paper is organized as follows: in Secs. II and III we describe the variational approach that we have employed; in Sec. IV, we present our numerical results. Finally, in Sec. V, we discuss the conclusions and the perspectives.

## II. VARIATIONAL METHOD

The variational approach is based on a Gutzwiller-projected fermionic wave function, which is constructed from an auxiliary superconducting (BCS) Hamiltonian:

$$\mathcal{H}_0 = \sum_{R,R',\sigma} t_{R,R'} c_{R,\sigma}^\dagger c_{R',\sigma} + \sum_{R,R'} \Delta_{R,R'} (c_{R,\uparrow}^\dagger c_{R',\downarrow}^\dagger + c_{R',\uparrow}^\dagger c_{R,\downarrow}^\dagger) + \text{H.c.} \quad (4)$$

Here,  $c_{R,\sigma}^\dagger$  ( $c_{R,\sigma}$ ) creates (destroys) an electron with spin  $\sigma = \pm 1/2$  on site  $R$ ;  $t_{R,R'}$  and  $\Delta_{R,R'}$  are hopping and singlet pairing terms, respectively. This Hamiltonian is quadratic in the fermionic operators and therefore can be easily diagonalized. Its ground state is denoted by  $|\Phi_0\rangle$ . Of course, this quantum state is not suitable to describe a spin system since it is defined in the “enlarged” Hilbert space with empty and doubly occupied sites. Then, a suitable variational wave function for the Heisenberg model of Eq. (3) can be obtained by projecting out all the configurations with at least one empty or doubly occupied site:

$$|\Psi_0\rangle = \mathcal{P}_G |\Phi_0\rangle, \quad (5)$$

where  $\mathcal{P}_G = \prod_R (n_{R,\uparrow} - n_{R,\downarrow})^2$  (with  $n_{R,\sigma} = c_{R,\sigma}^\dagger c_{R,\sigma}$  being the local electron density per spin  $\sigma$  on site  $R$ ) is the Gutzwiller projector, which enforces single fermionic occupation on each site. It has been shown that Gutzwiller-projected fermionic wave functions are very accurate for describing the exact ground state of the one-dimensional Heisenberg model with  $J_2 = 0$ , as well as the lowest-energy spinon excitations [35].

The parameters of  $\mathcal{H}_0$ , i.e., hopping and pairing amplitudes, are taken to be real and fully optimized by means of the stochastic reconfiguration technique in order to minimize the variational energy of  $|\Psi_0\rangle$  [36]. In most of the calculations, we will impose translational symmetry in the quadratic Hamiltonian  $\mathcal{H}_0$ , strongly reducing the number of independent parameters to be treated. We must emphasize the fact that both periodic boundary conditions (PBCs) and antiperiodic boundary conditions (APBCs) are allowed within the auxiliary BCS Hamiltonian (leading to a real wave function). However, while in the presence of a gapped fermionic spectrum either option will lead to a *unique* ground state, the same may not be true for a gapless spectrum. For example, if there are gapless points at  $k = \pm\pi/2$ , the ground state is unique if PBCs (APBCs) are considered for  $L = 4n + 2$  ( $L = 4n$ ), where  $n$  is an integer.

In order to tackle the problem of computing  $S^z(q, \omega)$ , we need to devise a way to construct excited states. Following the procedure of Ref. [31], we first introduce a set of *two-spinon* triplet excitations with momentum  $q$ , which are obtained by the

Gutzwiller projection of particle-hole fermionic excitations:

$$|q, R\rangle = \mathcal{P}_G \frac{1}{\sqrt{L}} \sum_{R'} e^{iqR'} \sum_{\sigma} \sigma c_{R+R',\sigma}^\dagger c_{R',\sigma} |\Phi_0\rangle. \quad (6)$$

Then, for each momentum  $q$ ,  $\{|q, R\rangle\}$  defines a (nonorthogonal) basis set that can be used to approximate the exact low-energy excitations. In other words, we can define a set of  $L$  states [37] (for each momentum  $q$ ), which are labeled by  $n$ :

$$|\Psi_n^q\rangle = \sum_R A_R^{n,q} |q, R\rangle. \quad (7)$$

The coefficients  $A_R^{n,q}$  are obtained by diagonalizing the Heisenberg Hamiltonian within the subspace generated by  $\{|q, R\rangle\}$  for each  $q$ , namely, by solving the generalized eigenvalue problem:

$$\sum_{R'} H_{R,R'}^q A_{R'}^{n,q} = E_n^q \sum_{R'} O_{R,R'}^q A_{R'}^{n,q}, \quad (8)$$

where we have introduced two matrices,  $H_{R',R}^q = \langle q, R' | \mathcal{H} | q, R \rangle$  (Hamiltonian) and  $O_{R',R}^q = \langle q, R' | q, R \rangle$  (overlap). Notice that, within our fermionic variational approach, the basis set  $\{|q, R\rangle\}$  provides a natural generalization of the well-known *single-mode approximation* [38] that is recovered by restricting ourselves to consider only  $|q, 0\rangle = S_q^z |\Psi_0\rangle$ .

Finally, the dynamical structure factor of Eq. (1) is approximated by taking

$$S^z(q, \omega) = \sum_n |\langle \Psi_n^q | S_q^z | \Psi_0 \rangle|^2 \delta(\omega - E_n^q + E_0^{\text{var}}), \quad (9)$$

where, compared to the exact form of Eq. (1), the variational states  $|\Psi_0\rangle$  and  $\{|\Psi_n^q\rangle\}$  are considered (instead of the exact eigenstates) and the variational energies  $E_0^{\text{var}}$  (corresponding to  $|\Psi_0\rangle$ ) and  $\{E_n^q\}$  are taken (instead of the exact ones). Most importantly, the sum over excited states runs over, at most,  $L$  states (instead of an exponentially large number). By using Eq. (7), we have

$$S^z(q, \omega) = \sum_n \left| \sum_R (A_R^{n,q})^* O_{R,0}^q \right|^2 \delta(\omega - E_n^q + E_0^{\text{var}}). \quad (10)$$

Remarkably, all the quantities that define the dynamical structure factor of Eq. (10) can be computed within a variational Monte Carlo scheme (i.e., without any sign problem). In fact, the entries of the Hamiltonian and overlap matrices are given by

$$H_{R',R}^q = \sum_x \langle q, R' | x \rangle \langle x | \mathcal{H} | q, R \rangle, \quad (11)$$

$$O_{R',R}^q = \sum_x \langle q, R' | x \rangle \langle x | q, R \rangle, \quad (12)$$

where  $\{|x\rangle\}$  is a set of normalized and orthogonal states, which can be sampled by using the variational wave function  $|\langle x | \Psi_0 \rangle|^2$  as the probability distribution:

$$H_{R',R}^q = \sum_x \left[ \frac{\langle q, R' | x \rangle \langle x | \mathcal{H} | q, R \rangle}{\langle \Psi_0 | x \rangle \langle x | \Psi_0 \rangle} \right] |\langle x | \Psi_0 \rangle|^2, \quad (13)$$

$$O_{R',R}^q = \sum_x \left[ \frac{\langle q, R' | x \rangle \langle x | q, R \rangle}{\langle \Psi_0 | x \rangle \langle x | \Psi_0 \rangle} \right] |\langle x | \Psi_0 \rangle|^2. \quad (14)$$

At this stage, it is worth making two remarks. First of all, our sampling procedure is possible because both the ground-state wave function  $|\Psi_0\rangle$  and the particle-hole excitations of Eq. (6) have  $S_{\text{tot}}^z = \sum_R S_R^z = 0$ , and therefore, the set of configurations  $\{|x\rangle\}$  can be chosen to also have  $S_{\text{tot}}^z = 0$ . This would not be possible when considering excitations involving a spin flip. For this case, a different sampling procedure was proposed in Ref. [31]. The most important advantage of our approach is that all the values of the momentum  $q$  can be computed with a *single* Monte Carlo simulation, at variance with the previous technique, in which each  $q$  needs a separate calculation. Second, within our formulation, the sampling is correct whenever the ground-state wave function  $\langle x | \Psi_0 \rangle$  is nonzero for all the configurations  $|x\rangle$ ; otherwise, the sampling procedure neglects the contributions from these “vanishing” configurations. We checked that, for most of the cases we considered, the number of these configurations is negligible, and therefore, they do not affect the final results.

We emphasize that, within this procedure, once the ground-state wave function is optimized, the only remaining parameters are the coefficients  $\{A_R^{n,q}\}$ , which are completely determined by solving Eq. (8). In other words, the particle-hole excitations are applied to a *fixed* reference state, i.e.,  $|\Phi_0\rangle$ , which is optimized, once for all, to minimize the ground-state variational energy.

The evaluation of  $O_{R',R}^q$  and  $H_{R',R}^q$  essentially boils down to computing the following quantities:

$$G_{R,R'}^\sigma(x) = \frac{\langle x | c_{R,\sigma}^\dagger c_{R',\sigma} | \Psi_0 \rangle}{\langle x | \Psi_0 \rangle}, \quad (15)$$

$$\Gamma_{R,R'}^\sigma(x) = \frac{\langle x | \mathcal{H} c_{R,\sigma}^\dagger c_{R',\sigma} | \Psi_0 \rangle}{\langle x | \Psi_0 \rangle}. \quad (16)$$

Once  $O_{R',R}^q$  and  $H_{R',R}^q$  have been evaluated, the generalized eigenvalue problem (8) for the excited states of momentum  $q$  can be solved. In doing so, we need to get rid of the linear dependence, which may affect the set  $\{|q, R\rangle\}$ . This is achieved by restricting Eq. (8) to the subspace of eigenvectors of the overlap matrix that have nonzero eigenvalues. In practice, since the entries  $O_{R',R}^q$  are computed stochastically, we need to discard the eigenvectors whose eigenvalues are smaller than some given tolerance.

### III. THE GROUND-STATE VARIATIONAL WAVE FUNCTION

The phase diagram of the one-dimensional  $J_1$ - $J_2$  Heisenberg model is well known [39]: for small values of the frustrating ratio, the system is gapless (i.e., a Luttinger fluid) with power-law spin-spin correlations, while for large values of  $J_2/J_1$ , the system is in a gapped phase characterized by long-range dimer order. In addition, (short-ranged) spin-spin correlations show an incommensurate periodicity for  $J_2/J_1 \gtrsim 0.5$ . The critical (Kosterlitz-Thouless) point that separates gapless and gapped phases has been estimated with high accuracy,  $(J_2/J_1)^c = 0.241167 \pm 0.000005$  [40].

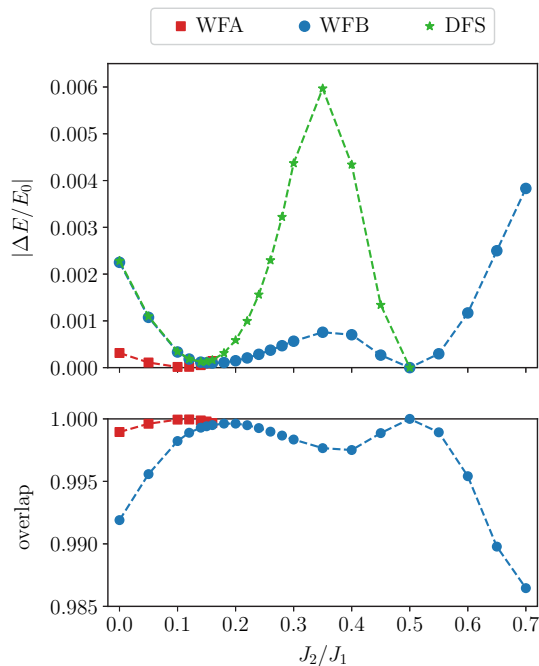


FIG. 1. Top: accuracy of the *DFS*, *WFA*, and *WFB* wave functions for a chain of  $L = 30$  sites.  $\Delta E$  is the difference between the variational energy  $E_0^{\text{var}}$  and the exact ground-state energy  $E_0$ , obtained with Lanczos diagonalizations. For  $J_2/J_1 > 0.5$ , the accuracy of the *DFS* state is not shown since it rapidly deteriorates. Bottom: overlap  $|\langle \Psi_0 | \Upsilon_0 \rangle|$  between the variational wave functions, either *WFA* or *WFB*, and the exact one.

The simplest *Ansatz* that can be used to describe both phases is the one obtained from a pure hopping Hamiltonian  $\mathcal{H}_0$  with broken translational symmetry. This can be achieved by doubling the unit cell and taking different intracell ( $t_1$ ) and intercell ( $t'_1$ ) hoppings. When  $t_1 = t'_1$ ,  $\mathcal{H}_0$  recovers translational invariance and reduces to the case of free fermions in one dimension, which have a Fermi sea ground state and gapless excitations. Instead, when  $t'_1 \neq t_1$ , there are two fermionic bands separated by a finite gap. The uniform and dimerized states are dubbed *UFS* and *DFS*, respectively. The accuracy for a cluster with  $L = 30$  sites is shown in the top panel of Fig. 1. For  $J_2/J_1 \lesssim 0.35$  the optimal wave function does not break the translational symmetry (i.e.,  $t'_1 = t_1$ ); by contrast, for larger

values of the frustrating ratio,  $t'_1 \neq t_1$ . At the Majumdar-Ghosh point ( $J_2/J_1 = 0.5$ ), one of the two hopping parameters is equal to zero, indicating that the wave function is a product of nearest-neighbor singlets. Here, the variational state becomes exact. Actually, the fully dimerized wave function remains the optimal solution for  $J_2/J_1 > 0.5$ , but its accuracy quickly worsens since its energy is independent of  $J_2$ .

More accurate wave functions can be built from translationally invariant *Ansätze*, which include both hopping and pairing terms (with  $t_{R,R'} = t_{|R-R'|}$  and  $\Delta_{R,R'} = \Delta_{|R-R'|}$ ). Nonetheless, even by considering translational symmetry, a “spontaneous symmetry breaking” mechanism is possible after Gutzwiller projection is included, leading, for example, to dimer order [41,42]. Within a gapless regime, an extremely accurate state, dubbed *WFA*, is constructed from a fermionic Hamiltonian that contains first- and third-neighbor hoppings ( $t_1$  and  $t_3$ ), as well as first-neighbor pairing  $\Delta_1$ . This choice gives a gapless fermionic band at  $k = \pm\pi/2$  and can be stabilized up to  $J_2/J_1 \approx 0.15$ . For larger values of the frustrating ratio, the pairing term goes to zero, and the wave function coincides with the *UFS* state. A different possibility, which allows the existence of a gap in the fermionic spectrum, is given by taking first-neighbor hopping and both on-site ( $\Delta_0$ ) and second-neighbor ( $\Delta_2$ ) pairings. This *Ansatz*, which is dubbed *WFB*, is gapped unless  $\Delta_0 = -\Delta_2$ . Optimizing the parameters of this wave function for  $L = 30$  sites, we find that it reduces to the simple *UFS* state (i.e.,  $\Delta_0 = \Delta_2 = 0$ ) for  $J_2/J_1 \lesssim 0.1$ . Then, the optimal pairing terms become nonzero, and the wave function proves to be more accurate than the *DFS* state and stable for all the values of the frustrating ratios (see Fig. 1).

We expect that, in the thermodynamic limit, the gap in the fermionic spectrum will open in the vicinity of the exact transition point  $(J_2/J_1)^c$  and will follow the behavior of the spin gap. However, it is extremely hard to locate this point by performing a finite-size-scaling analysis since the gap is exponentially small in an extended region after the critical point.

#### IV. RESULTS

Here, we present the numerical results for the spin structure factor of a one-dimensional chain. Let us start by considering a small cluster with  $L = 30$  sites, where exact diagonalizations are possible using the Lanczos method. First of all, we

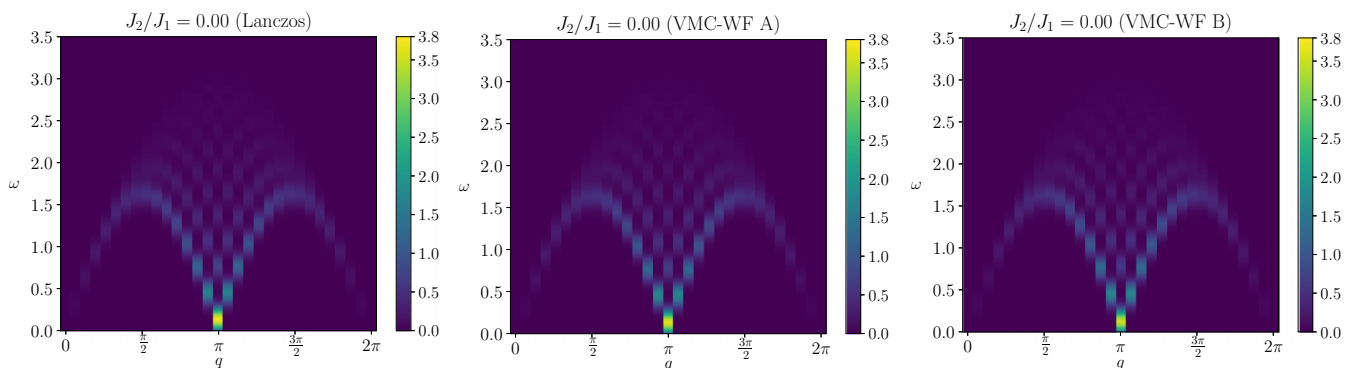


FIG. 2. Dynamical structure factor for  $L = 30$  and  $J_2 = 0$ . The Lanczos results are reported in the left panel. The variational calculations in the middle and right panels were obtained using the *Ansätze* *WFA* and *WFB*, respectively.

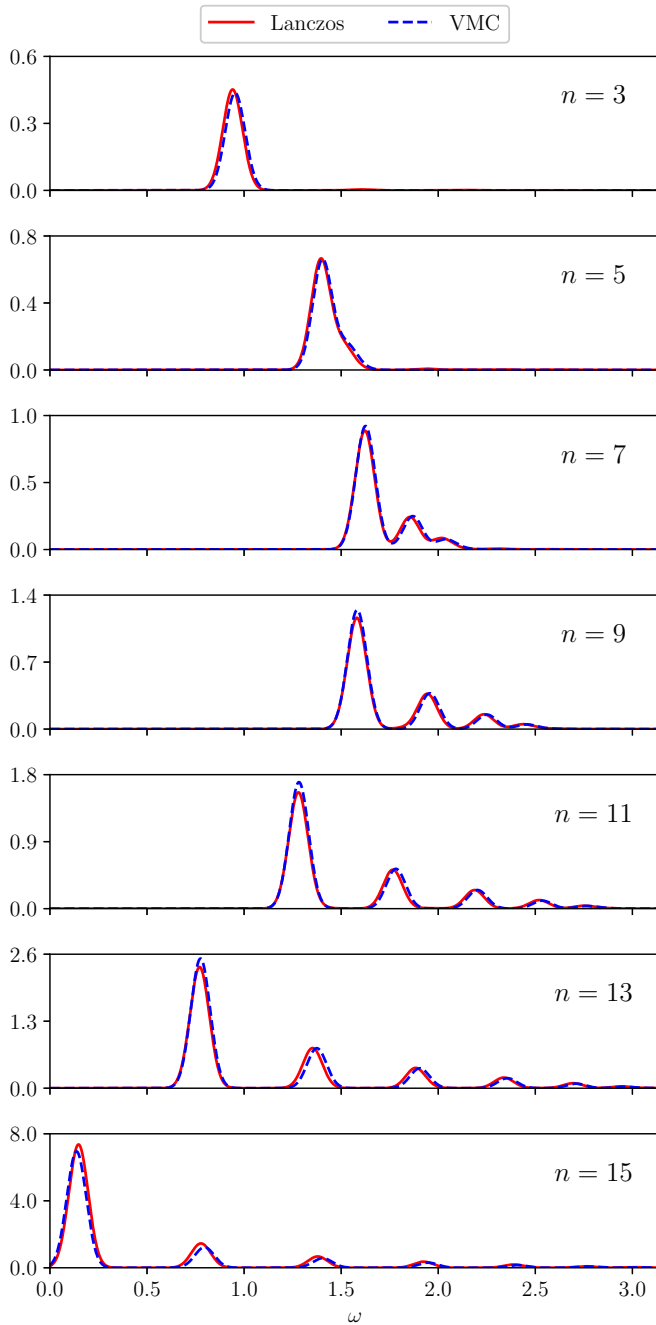


FIG. 3. Comparison between Lanczos and variational calculations for  $S^z(q, \omega)$  at different momenta  $q = 2\pi/L \times n$ , with  $n$  being an integer specified in the figure. Here, we consider  $L = 30$  and  $J_2 = 0$ . The  $\delta$  functions in Eqs. (1) and (9) have been replaced by normalized Gaussians with  $\sigma = 0.05J_1$ . Statistical errors are negligible within the present scale.

demonstrate that the variational results do not change appreciably when considering the wave function *WFA* or *WFB* to compute the dynamical structure factor (see Fig. 2). Indeed, even though the latter state is about five times less accurate than the former one for  $J_2 = 0$  (see Fig. 1), the actual differences between the two dynamical calculations are negligible (and either option gives an excellent description of the exact results). Therefore, in the following, we consider only the *WFB* wave function to compute the dynamical structure factor.

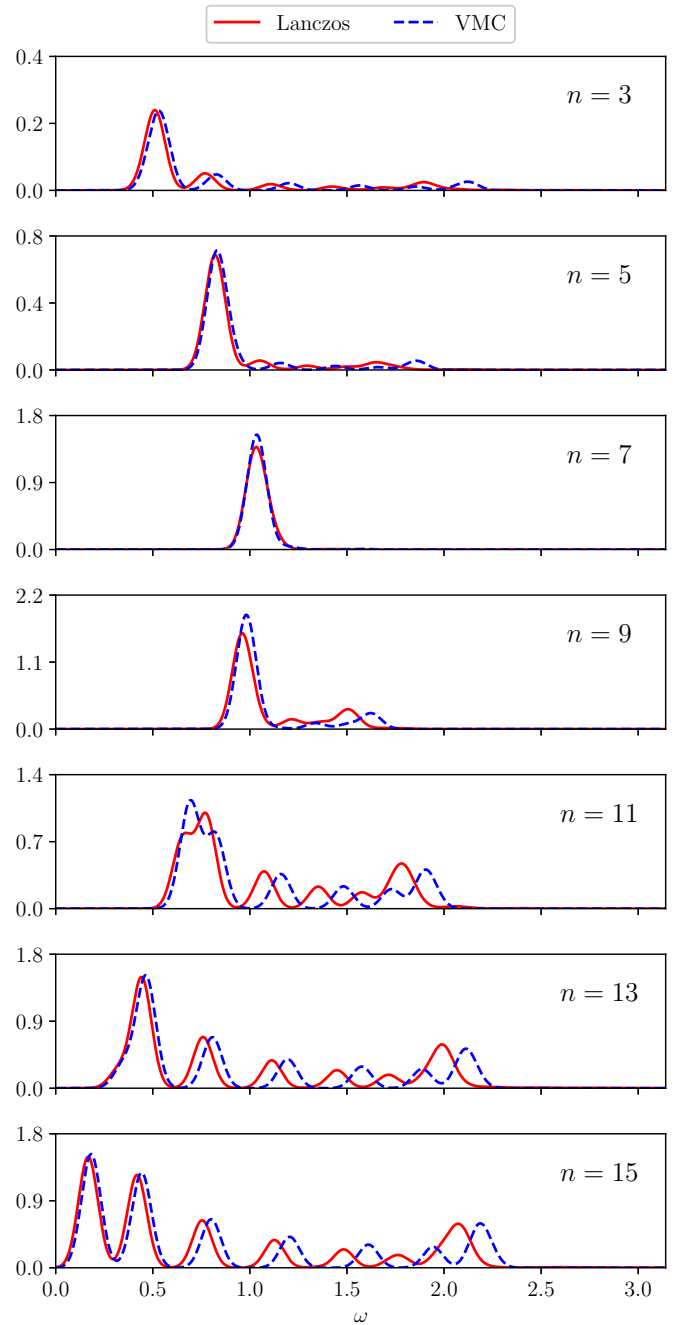


FIG. 4. The same as in Fig. 3, but for  $J_2/J_1 = 0.45$ .

In order to best quantify the agreement between the variational and the exact calculations, we directly report  $S^z(q, \omega)$  for several momenta  $q$  as a function of the frequency  $\omega$  for two values of the frustrating ratio,  $J_2/J_1 = 0$  and  $0.45$  (see Figs. 3 and 4). Here, the  $\delta$  functions related to the exact and variational energies entering Eqs. (1) and (9) have been replaced by normalized Gaussians with  $\sigma = 0.05J_1$ . The agreement is very good not only for the unfrustrated case with  $J_2 = 0$  (see Fig. 3) but also in the presence of a sizable frustration,  $J_2/J_1 = 0.45$  (see Fig. 4). Similar results are also obtained for larger values of the ratio  $J_2/J_1$  (see below). Therefore, it is expected that, within this approach, both gapless and gapped regimes are correctly described. The accuracy of the variational method is

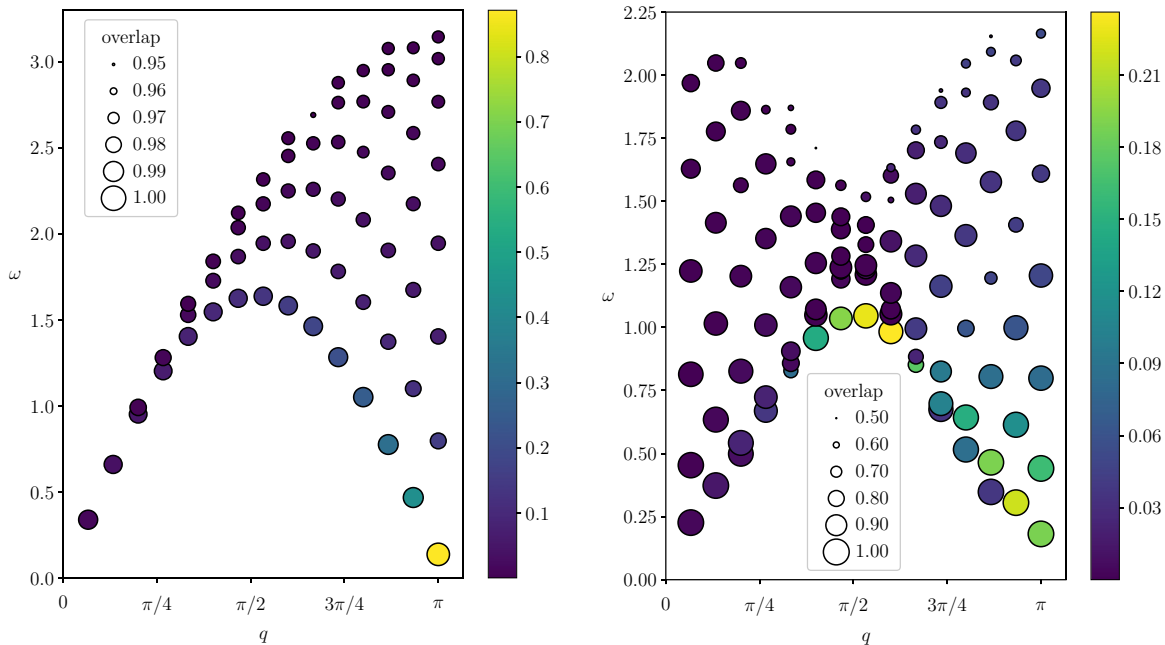


FIG. 5. The overlaps between the exact and the variational excitations are reported for a chain of  $L = 30$  sites. The cases with  $J_2 = 0$  (left panel) and  $J_2/J_1 = 0.45$  (right panel) are shown. The size of the circles indicates the magnitude of the overlap, while their colors represent the value of the variational spectral weights  $|\langle \Psi_n^q | S_q^z | \Psi_0 \rangle|^2$ . For a detailed description of the calculations of the overlaps, see the main text.

highlighted in Fig. 5, where we report the overlaps between the variational excited states of Eq. (7) and the exact ones. In particular, whenever the excited states are well separated in energy, it is easy to match each exact excitation with a corresponding variational one (in this case, the overlap is very large, as for  $J_2 = 0$ ). Instead, when two or even more excitations are close in energy, this correspondence is not easy to resolve and, for each variational state, we computed the overlap with all the exact states and plotted the maximum value. In this case, a reduction in the overlap is observed, as for a number of cases at  $J_2/J_1 = 0.45$ . Nevertheless, in all cases, the relevant excitations, which carry sizable spectral weight, are well reproduced by the variational approach, and a reduced overlap is detected for states which do not contribute much to the whole intensity of the dynamical structure factor.

Finally, the results obtained with the exact and variational approaches are compared in Fig. 6, where  $S^z(q, \omega)$  of a chain of  $L = 30$  sites is represented using color maps for  $J_2/J_1 = 0.2, 0.45, 0.7$ , and 1. In all the cases, the variational results follow the exact ones, including the development of incommensurate features when  $J_2/J_1 > 0.5$ . In fact, by increasing the frustrating ratio, the intensity progressively shifts from  $q = \pi$  (low energies) to  $q = \pm\pi/2$  (high energies). At even larger values of  $J_2/J_1$ , the modes at  $q = \pm\pi/2$  soften and eventually become gapless for  $J_2 \rightarrow \infty$  (in this limit, the spin Hamiltonian consists of two decoupled Heisenberg models, one for each sublattice, and  $J_2$  represents a nearest-neighbor superexchange on each sublattice). Remarkably, the variational approach is able to perfectly reproduce all the relevant features of the dynamical structure factor. Moreover, we find that the sum rule

$$\int d\omega S^z(q, \omega) = \langle \Psi_0 | S_{-q}^z S_q^z | \Psi_0 \rangle \quad (17)$$

is satisfied within the error bars for all the values of the frustrating ratio considered here. We mention the fact that the only case where our sampling technique fails is at the Majumdar-Ghosh point  $J_2/J_1 = 0.5$ , where the number of vanishing configurations in the ground-state wave function (exactly reproduced by our Gutzwiller-projected fermionic state) is exponentially large.

The results for a large cluster with  $L = 198$  sites are reported in Fig. 7 for  $J_2/J_1 = 0, 0.2, 0.4, 0.45, 0.7$ , and 1. In the unfrustrated case, it is known [22] that most of the total intensity of the dynamical structure factor is carried by the two-spinon contributions. For these excitations the lower and upper energy limits are given by

$$\omega_{\text{lower}} = \frac{\pi}{2} |\sin(q)|, \quad (18)$$

$$\omega_{\text{upper}} = \pi \left| \sin\left(\frac{q}{2}\right) \right|. \quad (19)$$

Indeed, we find that our dynamical structure factor is bounded by these limits and closely resembles the one that has been recently obtained with a Bethe *Ansatz* approach [20,24].

It should be stressed that, for a relatively large region within the gapped phase, the value of the spin gap remains very small since the transition from the gapless to the dimerized phase belongs to the Kosterlitz-Thouless universality class. Therefore, even for a relatively large system size, it is very hard to detect the presence of a finite gap in the excitation spectrum: for example, the dynamical structure factors at  $J_2/J_1 = 0.2$  and 0.4 (see Fig. 7) look very similar, even though the former case corresponds to a gapless phase and the latter corresponds to a gapped spectrum. On this large cluster, the gradual shift of the intensity from  $q = \pi$  to  $q = \pm\pi/2$  is evident, as well as the presence of a “rounding” around  $q = \pi$

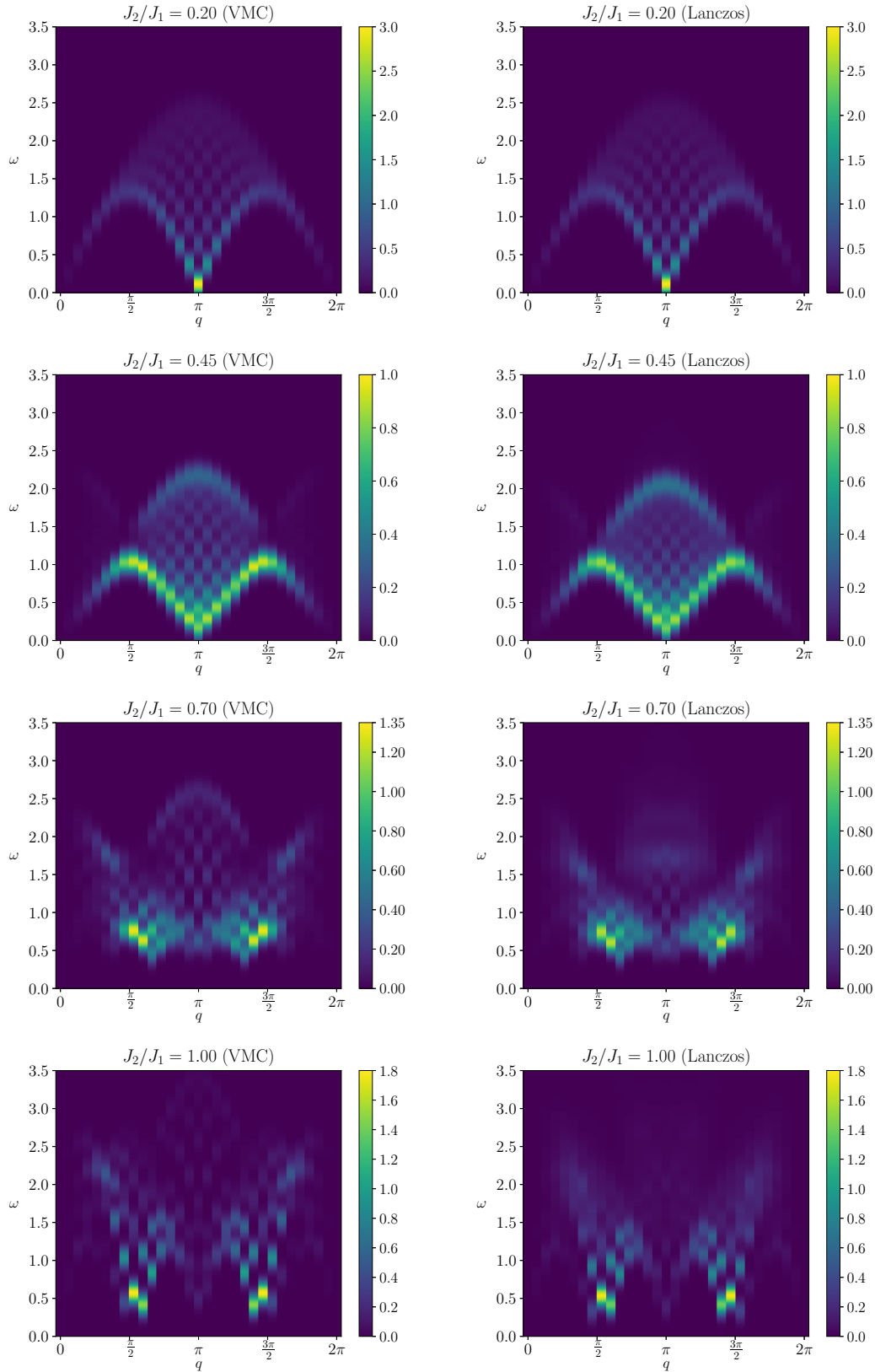


FIG. 6. Dynamical spin structure factor  $S^z(q, \omega)$  for a chain of  $L = 30$  sites: comparison of variational and Lanczos results for different values of the frustrating ratio. The  $\delta$  functions in Eqs. (1) and (9) have been replaced by normalized Gaussians with  $\sigma = 0.1 J_1$ .

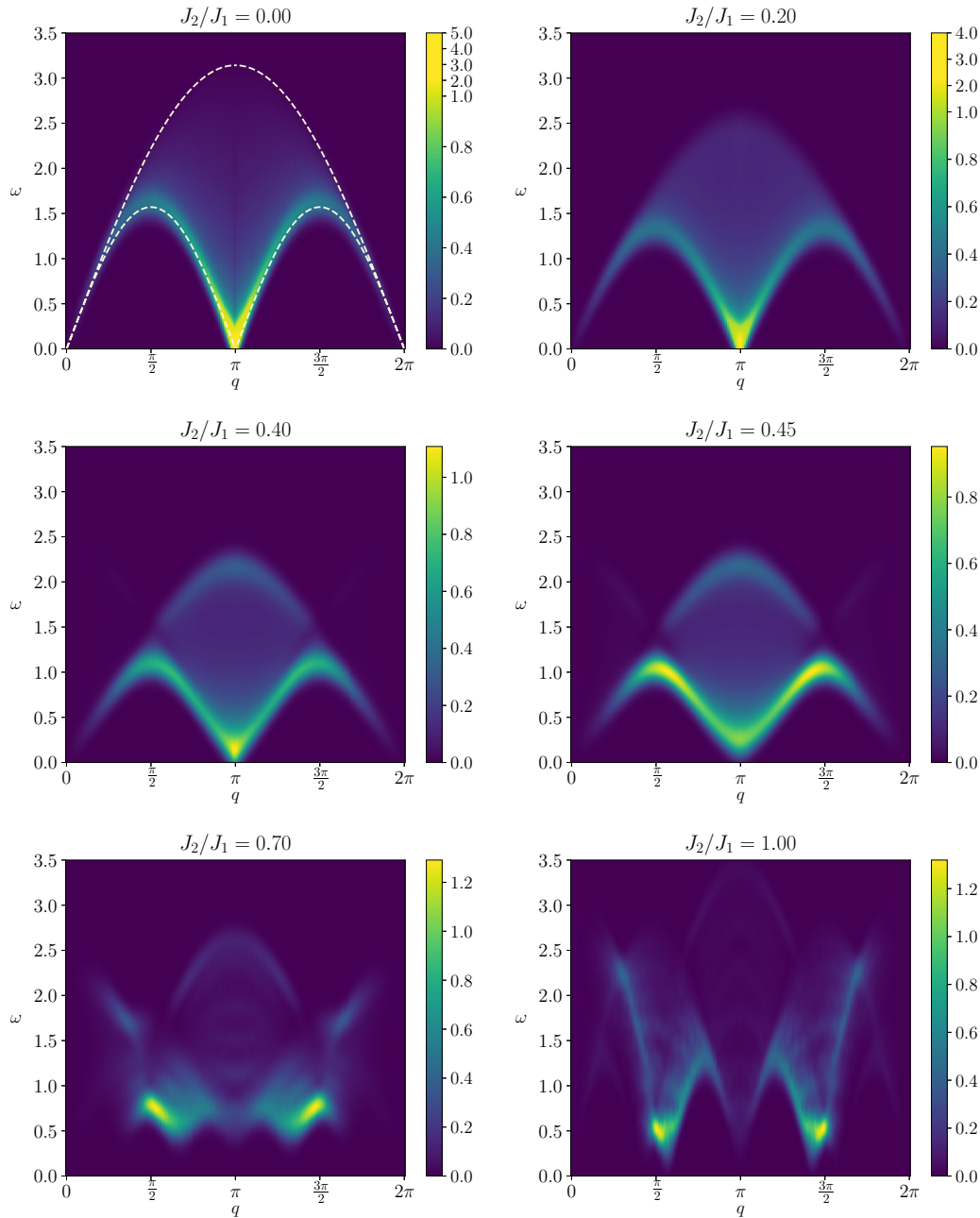


FIG. 7. Dynamical spin structure factor  $S^z(q, \omega)$  for different values of the frustrating ratio and  $L = 198$  sites. The  $\delta$  functions in Eq. (9) have been replaced by normalized Gaussians with  $\sigma = 0.1J_1$ . The white dashed lines for  $J_2 = 0$  indicate the lower and upper limits of the two-spinon contributions, Eqs. (18) and (19).

within the gapped phase for  $J_2/J_1 < 0.5$ . Within such a large size, incommensurate features appear clearly for  $J_2/J_1 > 0.5$ ; namely, the excitations with lowest energy move from  $q = \pi$  to  $q = \pm\pi/2$ , giving rise to a nontrivial form of the spectral function. These effects are determined by the gapped BCS spectrum, whose minima lie at incommensurate momenta. The rich structure of  $S^z(q, \omega)$  is related to the fact that, in the limit  $J_2/J_1 \rightarrow \infty$ , the system decouples into two independent Heisenberg chains with coupling constant  $J_2$ . The Brillouin zone is then halved with respect to the case with  $J_2 = 0$ , and the dynamical structure factor is given by the repetition of the one of the pure Heisenberg model between  $[0, \pi]$  and  $[\pi, 2\pi]$ , scaled by  $J_2/J_1$ . For finite values of  $J_2/J_1$  in the

incommensurate phase, the spectral features at high energies are related to the lower and upper bounds of the two-spinon continuum that develops in the aforementioned limit.

### V. CONCLUSIONS

In conclusion, we have used a variational approach to study the dynamical spin structure factor of the frustrated  $J_1$ - $J_2$  model in one spatial dimension. Here, excitations at a given momentum  $q$  are directly constructed from a Gutzwiller-projected fermionic wave function, thus avoiding any sign problem and/or analytic continuation from imaginary or real times to frequencies. In contrast to the original definition where

these excitations have  $S^z = 1$  [31], here, we have considered states with  $S^z = 0$ , which allow us to have a much simpler Monte Carlo sampling. Indeed, within our technique, the dynamical structure factor  $S^z(q, \omega)$  can be computed for all momenta  $q$  within a *single* Monte Carlo simulation.

We have reported the unprecedented accuracy of this method not only at or close to the integrable point with  $J_2 = 0$  but also for generic values of the frustrating ratio. The remarkable advantage of this variational procedure is given by the fact that the relevant part of the low-energy spectrum can be described by considering particle-hole excitations on top of a fixed “reference” state. Indeed, once the variational wave function has been optimized for the ground state, only  $O(L)$  parameters for each  $q$  are used to reproduce the low-

energy part of the spectrum. This fact suggests that Gutzwiller-projected fermionic wave functions not only may accurately reproduce the ground-state properties of frustrated spin models but also constitute a good framework to generate low-energy excitations.

This work shows that the present variational approach to compute the dynamical structure factor is very promising, especially in the case of two-dimensional frustrated spin models, for which a straightforward generalization is possible. The reliability of the results for different (gapped and gapless) phases and the possibility to consider relatively large sizes make this method very suitable not only for theoretical investigations of other spin models but also for direct comparisons with neutron-scattering experiments.

- 
- [1] L. Balents, *Nature (London)* **464**, 199 (2010).
- [2] L. D. Faddeev and L. A. Takhtajan, *Phys. Lett. A* **85**, 375 (1981).
- [3] L. Pitaevskii and S. Stringari, *J. Low Temp. Phys.* **85**, 377 (1991).
- [4] F. D. M. Haldane, *Phys. Rev. Lett.* **60**, 635 (1988); B. S. Shastry, *ibid.* **60**, 639 (1988).
- [5] F. D. M. Haldane, *Phys. Rev. Lett.* **66**, 1529 (1991).
- [6] C. K. Majumdar and D. Ghosh, *J. Math. Phys.* **10**, 1388 (1969).
- [7] B. S. Shastry and B. Sutherland, *Phys. Rev. Lett.* **47**, 964 (1981).
- [8] A. Kitaev, *Ann. Phys. (N.Y.)* **321**, 2 (2006).
- [9] See, for example, C. Lacroix, P. Mendels, and F. Mila, *Introduction to Frustrated Magnetism Materials, Experiments, Theory* (Springer, Berlin, 2013).
- [10] S. Yan, D. A. Huse, and S. R. White, *Science* **332**, 1173 (2011).
- [11] S. Depenbrock, I. P. McCulloch, and U. Schollwöck, *Phys. Rev. Lett.* **109**, 067201 (2012).
- [12] Y. Iqbal, D. Poilblanc, and F. Becca, *Phys. Rev. B* **89**, 020407(R) (2014).
- [13] A. M. Läuchli, J. Sudan, and R. Moessner, [arXiv:1611.06990](https://arxiv.org/abs/1611.06990).
- [14] W. T. Fuhrman, M. Mourigal, M. E. Zhitomirsky, and A. L. Chernyshev, *Phys. Rev. B* **85**, 184405 (2012).
- [15] M. Mourigal, W. T. Fuhrman, A. L. Chernyshev, and M. E. Zhitomirsky, *Phys. Rev. B* **88**, 094407 (2013).
- [16] E. A. Ghioldi, M. G. Gonzalez, S. Zhang, Y. Kamiya, L. O. Manuel, A. E. Trumper, and C. D. Batista, [arXiv:1802.06878](https://arxiv.org/abs/1802.06878).
- [17] M. E. Zhitomirsky and A. L. Chernyshev, *Rev. Mod. Phys.* **85**, 219 (2013).
- [18] R. Coldea, S. M. Hayden, G. Aeppli, T. G. Perring, C. D. Frost, T. E. Mason, S.-W. Cheong, and Z. Fisk, *Phys. Rev. Lett.* **86**, 5377 (2001).
- [19] H. M. Rønnow, D. F. McMorrow, R. Coldea, A. Harrison, I. D. Youngson, T. G. Perring, G. Aeppli, O. Syljuåsen, K. Lefmann, and C. Rischel, *Phys. Rev. Lett.* **87**, 037202 (2001).
- [20] B. Lake, D. A. Tennant, J.-S. Caux, T. Barthel, U. Schollwöck, S. E. Nagler, and C. D. Frost, *Phys. Rev. Lett.* **111**, 137205 (2013).
- [21] F. D. M. Haldane and M. R. Zirnbauer, *Phys. Rev. Lett.* **71**, 4055 (1993).
- [22] M. Karbach, G. Müller, A. H. Bougourzi, A. Fledderjohann, and K.-H. Mütter, *Phys. Rev. B* **55**, 12510 (1997).
- [23] J.-S. Caux and J. M. Maillet, *Phys. Rev. Lett.* **95**, 077201 (2005).
- [24] J.-S. Caux and R. Hagemans, *J. Stat. Mech.* (2006) P12013.
- [25] J. Knolle, D. L. Kovrizhin, J. T. Chalker, and R. Moessner, *Phys. Rev. Lett.* **112**, 207203 (2014); *Phys. Rev. B* **92**, 115127 (2015).
- [26] H. Yokoyama and Y. Saiga, *J. Phys. Soc. Jpn.* **66**, 3617 (1997).
- [27] A. Lavarélo and G. Roux, *Eur. Phys. J. B* **87**, 229 (2014).
- [28] T. Barthel, U. Schollwöck, and S. R. White, *Phys. Rev. B* **79**, 245101 (2009).
- [29] L. Vanderstraeten, J. Haegeman, F. Verstraete, and D. Poilblanc, *Phys. Rev. B* **93**, 235108 (2016).
- [30] H. D. Xie, R. Z. Huang, X. J. Han, X. Yan, H. H. Zhao, Z. Y. Xie, H. J. Liao, and T. Xiang, *Phys. Rev. B* **97**, 075111 (2018).
- [31] T. Li and F. Yang, *Phys. Rev. B* **81**, 214509 (2010).
- [32] A variational computation of excited states (avoiding analytical continuation) has also been proposed within a matrix-product state approach; see L. Vanderstraeten, F. Verstraete, and J. Haegeman, *Phys. Rev. B* **92**, 125136 (2015).
- [33] B. Dalla Piazza, M. Mourigal, N. B. Christensen, G. J. Nilsen, P. Tregenna-Piggott, T. G. Perring, M. Enderle, D. F. McMorrow, D. A. Ivanov, and H. M. Rønnow, *Nat. Phys.* **11**, 62 (2015).
- [34] J.-W. Mei and X.-G. Wen, [arXiv:1507.03007](https://arxiv.org/abs/1507.03007).
- [35] S. Yunoki and S. Sorella, *Phys. Rev. B* **74**, 014408 (2006).
- [36] S. Sorella, *Phys. Rev. B* **71**, 241103(R) (2005).
- [37] In many cases, the set of states  $\{|q, R\rangle\}$  is linearly dependent. This reduces the effective number of excitations  $|\Psi_n^q\rangle$  which can be constructed.
- [38] See, for example, A. Auerbach, *Interacting Electrons and Quantum Magnetism* (Springer, New York, 1994).
- [39] S. R. White and I. Affleck, *Phys. Rev. B* **54**, 9862 (1996).
- [40] S. Eggert, *Phys. Rev. B* **54**, R9612 (1996).
- [41] F. Becca, L. Capriotti, A. Parola, and S. Sorella, in *Introduction to Frustrated Magnetism: Materials, Experiments, Theory*, edited by C. Lacroix, P. Mendels, and F. Mila, Springer Series in Solid-State Sciences (Springer, Berlin, 2011), p. 379.
- [42] R. Kaneko, L. F. Tocchio, R. Valenti, F. Becca, and C. Gros, *Phys. Rev. B* **93**, 125127 (2016).